European Journal of Pharmaceutics and Biopharmaceutics 141 (2019) 90–99

Contents lists available at ScienceDirect

European Journal of Pharmaceutics and Biopharmaceutics

journal homepage: www.elsevier.com/locate/ejpb

Research paper

# Real-time monitoring of particle size distribution in a continuous granulation and drying process by near infrared spectroscopy

Victoria Pauli[a,b], Yves Roggo[b], Peter Kleinebudde[a], Markus Krumme[b,*]

[a] Institute of Pharmaceutics and Biopharmaceutics, Heinrich Heine University, Universitaetsstr. 1, 40225 Dusseldorf, Germany
[b] Novartis AG, 4002 Basel, Switzerland

ARTICLE INFO

*Keywords:*
Near infrared spectroscopy
Continuous manufacturing
Continuous granulation and drying
Particle size distribution
Process control
PAT

ABSTRACT

In continuous granulation, it can be important to control granules particle size distribution (PSD), as it may affect final product quality. Near infrared spectroscopy (NIRS) is already a routine analytical procedure within pharmaceutical continuous manufacturing for the in-line analysis of chemical material-characteristics. Consequently, the extraction of additional information related to granules' physical properties like particle size distribution is tempting, as it would enhance process knowledge without the need for new capital investments.

Three in-line NIRS methods were developed via partial least squares regression, to predict dried granules PSD-fractions X10, X50, and X90 within a GMP-qualified continuous twin-screw wet granulation and fluid-bed drying process. Methods were developed for the size range of 20–234 µm (X10), 98–1017 µm (X50), and 748–2297 µm (X90) and assessed with one internal and three external validation datasets in agreement with current guidelines on NIRS. Internal validation indicated root mean square error of predictions (RMSEPs) of 17 µm, 97 µm, and 174 µm, for PSD X10, X50, and X90 respectively, with acceptable linearity, slope, and bias. Furthermore, the ratio of prediction to deviation (RPD), the ratio of prediction error to laboratory error (PRL), and the range error ratio (RER) were evaluated, with all values within the acceptance range for adequate to good NIR methods ($1.75 > RPD < 3$, $PRL \leq 2$, $RER \geq 10$). Methods applicability to in-line processes and their robustness towards water content and active pharmaceutical ingredient content was further demonstrated with three independent in-line datasets in real-time, showing good agreement between predicted and reference values. In summary, methods demonstrated to be sufficient for their intended purpose to monitor trends and sudden changes in dried granules PSD during continuous granulation and drying. Because of their fast response time, they are unique tools to characterize the dynamic behavior and navigate the agglomeration state of the material in static and transient process conditions during continuous granulation and drying.

## 1. Introduction

Granulation of powder blends is a standard procedure in pharmaceutical manufacturing of solid oral dosage forms. It improves the processability of fine powders by increasing bulk density and flowability, which in turn reduces the risk for segregation of powder components and increases dispensing performance. As such it locks the ratio of active pharmaceutical ingredient (API) and excipients on a microscopic scale and hence is a helpful tool to ensure blend uniformity, especially in low strength dosages [1]. Common granulation methods include fluidized bed granulation, spray drying, extrusion, roller compaction, or high shear granulation. A drying step follows the granulation, if a liquid binder was used during granulation [2]. In recent years, pharmaceutical processing has evolved from traditional batch processing towards continuous manufacturing, as it has proven favorable in regard to process scale-up, process control and -economics as well as product quality [3]. In the course of this development, continuous twin-screw granulation (TSG) was established as an advanced high-shear granulation approach. In TSG, the powder blend of API and excipients is continuously fed into a barrel containing a set of co-rotating screws. Simultaneously, the granulation liquid is added at a predefined stoichiometric relationship to the powder mixture. The

*Abbreviations:* API, active pharmaceutical ingredient; CM, Continuous Manufacturing; LOD, loss-on-drying; NIRS, Near Infrared Spectroscopy; PAT, process analytical technology; PCA, principal component analysis; PLSR, partial least squares regression; PRL, ratio of prediction error to laboratory error; PSD, particle size distribution; RER, range error ratio; RMSECV, root mean square error of cross validation; RMSEP, root mean square error of prediction; RPD, ratio of prediction to deviation; SEL, standard error laboratory; TSG, twin-screw granulation

* Corresponding author at: Novartis Pharma AG, WSJ-27.1.015.01, Continuous Manufacturing (CM) Unit, CH-4002 Basel, Switzerland.
*E-mail address:* markus.krumme@novartis.com (M. Krumme).

https://doi.org/10.1016/j.ejpb.2019.05.007
Received 13 July 2018; Received in revised form 26 April 2019; Accepted 9 May 2019
Available online 10 May 2019
0939-6411/ 

high-shear forces applied by the rotating screws result in thorough mixing and formation of wet granules, while the material travels through the barrel. Granule properties can be adjusted by the liquid-to-solid ratio, the screw design, screw speed, and the formulation itself [4]. Commonly, the twin-screw granulator connects to a continuous fluid-bed dryer, where wet granules are dried before being compressed into tablets [3,5]. Variations in granules particle size distribution (PSD) can potentially cause issues in subsequent processing steps and affect the final product quality. For example, formation of too many fines can cause sticking on the tablet press, result in non-uniform drug content due to segregation, or alter the tablets disintegration and dissolution profiles. Simultaneously, too many oversized particles can alter the granules drying profiles; too wet material can cause issues during tableting and adversely affect tablet shelf life. Consequently, monitoring and control of PSD, can be an important aspect in continuous twin-screw granulation and drying, especially if the process demonstrated susceptibility to PSD variations [6].

Literature describes numerous options to monitor granules particle size in-line, at-line, or offline. Imaging techniques, focused beam reflectance, or spatial filter velocimetry are the most common methods for in-line or at-line analysis [7–9]. Drawbacks are the need for new equipment that has to be purchased, integrated into the process line, trained, qualified, and maintained. In this context, monitoring of particle size related information by near infrared spectroscopy (NIRS) has raised interest, as NIRS is already a widespread technique within continuous manufacturing for the monitoring of water content (specified as loss-on-drying, LOD) and API content [10–13]. NIRS allows rapid, non-destructive in-line analysis of the product stream in real-time, by investigating the vibrational properties of a sample in regard to the spectral wavelength applied. Spectral changes in specific NIR-regions are commonly attributed to chemical properties of the sample (e.g. API content) that allow qualitative and quantitative prediction of chemical sample features after appropriate chemometric calibration [9,14]. Furthermore, changes in the baseline and slope of a spectrum are thought to be related to physical sample properties like granule morphology, density, shape and size. In this case, chemometric calibration becomes more complex, as physical sample features can influence NIR-absorption patterns in numerous ways. For example, it was demonstrated before that larger particles allow deeper penetration of NIR radiation [7]. This in turn increases radiation absorption and causes baseline drifts. However, water on the granule surface may have a similar effect by absorbing more NIR radiation then a dry particle of the same size [7,9,10,14,15]. Hence, careful interpretation of these effects and thorough method validation is required.

Numerous approaches to correlate NIR spectra to physical sample characteristics related to particle size of wet granulation and drying processes were published in literature before. Early methods focused on calibrating single wavelength absorptions to particle size related information, like median granule size, but methods lacked the ability for quantitative prediction. Later methods improved in predictability, but accuracy diminished with small particles, the methods robustness against LOD was poor, or methods were merely developed and validated with offline data [10,16,17]. Rosas et al. [18] developed NIRS methods to quantify proportions of three particle size fractions (< 125 μm, 125–250 μm, > 250 μm) within a batch of granules. However, measurement was done after granulation, during a subsequent blending step, making real-time process control impossible. Otsuka et al. [19] successfully calibrated baseline offset to mean particle size and achieved reliable prediction of test samples, method development and validation however was done offline on lab-scale equipment. Tok et al. [20] correlated the absorption intensity at a single wavenumber to particle size fraction X50 in-line, but encountered problems with probe fouling. Nieuwmeyer et al. [11] calibrated in-line NIR spectra to median granule size during small-scale batch fluid-bed drying of lactose granules for end-point detection. As the model was developed with fully dried granules, the authors demonstrated no robustness towards varying LOD. To the authors best knowledge, only Alcalà et al. [13] demonstrated accurate prediction of three particle size fractions (< 125 μm, 125–1000 μm, > 1000 μm) by NIRS on a production scale industrial fluid-bed granulation process. However, manufacturing was done in batch mode.

In this study, development and validation of three in-line NIRS methods, that can accurately predict dried granules' PSD-fractions X10, X50, and X90 of a continuous twin-screw wet-granulation and fluid-bed drying process in real-time is presented. The methods were assessed with an internal validation dataset in compliance to common guidelines on validation of NIRS methods [21–25]. Furthermore, accuracy and robustness against dried granules' LOD and API content was demonstrated with three external datasets in real-time. The described granulation and drying units are part of a highly innovative, fully continuous, from powder-to-tablet, GMP-qualified manufacturing plant, dedicated to the production of solid oral dosage forms. A qualified NIR-spectrometer was already in place to monitor dried granules LOD and API content at the outlet of the continuous fluid-bed dryer. Consequently, employing a NIRS-method to monitor dried granules' PSD in real-time at the dryer outlet does not require any new equipment investments, while increasing process understanding. The methods intend to monitor trends and sudden changes in granules PSD, to complement the already established control strategy on dry granules moisture content (LOD) of the CM production line, as previously published in [4,26].

## 2. Materials and methods

### 2.1. Materials

Diclofenac Sodium (Acros Organics, Geel, Belgium) served as model compound in all trials. The formulation contained 25% Diclofenac Sodium, 5% Sodium Stearyl Fumarate (SPI Pharma, Inc., Wilmington, USA), 4% Hypromellose (Cellulose-HP-M 603) (Dow chemical company, West Drayton, UK), 5% Sodium Starch-Glycolate, 12.2% Calcium Hydrogen-Phosphate Anhydrous, and 48.8% Microcrystalline Cellulose PH102 (all from JRS Pharma, Rosenberg, Germany).

To generate granules varying in Diclofenac Sodium content, formulations containing 70–130% of the original drug content (i.e. 20–30% Diclofenac Sodium absolute) were prepared. In this case, the amounts of Hypromellose and Calcium Hydrogen-Phosphate Anhydrous were adapted accordingly, while keeping their ratio constant at 80:20. Purified water served as granulation liquid.

### 2.2. Preparation of powder blends

Batch size varied depending on the experiment between 5, 23, and 100 kg. For batch sizes of 5 kg, all ingredients were weighted into a 20L drum and blended two times for 5 min at 20 rpm with a Turbula Mixer (T10B, WAB AG Maschinenfabrik, Muttenz, Switzerland). For batch sizes of 23 kg (in a 100 L container) and 100 kg (in a 300 L container), blending was done twice for 10 min at 11 rpm in a Pharma Telescope Blender PTM 300 (LB Bohle GmbH, Ennigerloh, Deutschland). Between the two blending steps, the blend was sieved through a 1.25 mm-mesh sieve to break agglomerates and to ensure homogeneous distribution of all functional excipients.

### 2.3. Twin-screw wet-granulation

Continuous wet-granulation was performed on a Thermo Fisher Pharma 16 Twin Screw Granulator (TSG) (Thermo Fisher Scientific, Karlsruhe, Germany) with screw diameter (D) of 16 mm and a total screw length of 53 ¼ x D. Screw configuration was as follows (from inlet to outlet of the barrel): 2 D Feed Screw Elements (FSE), 2 D Long Helix Feed Screws, 22 D FSE, 2 ¼ D 30° Mixing Element, 22 D FSE, 3 D Distributive Feed Screw Elements. The powder blend was fed through the first feeding port in the barrel by a loss-in-weight powder feeder (K-

Tron T20, Coperion K-Tron GmbH, Niederlenz, Switzerland). Granulation liquid at room temperature was fed through the second port of the TSG-barrel by a custom made dispensing pump system (based on Watson Marlow, Zollikon, Switzerland) through a nozzle of 2.5 mm inner diameter. Feeder-calibration was performed each day by the feeder's internal calibration modes. Feeders were refilled manually, before the hopper-fill level decreased by more than 50%. Liquid feed rate was varied, to generate granules varying in PSD (at constant solid feed rate and drying conditions; see Section 2.6 for details). Standard process parameters are listed in Section 2.5.

### 2.4. Continuous fluid-bed drying

Continuous fluid-bed drying of wet granules was performed on a Glatt GPCG 2 CM fluid-bed dryer (Glatt GmbH, Binzen, Germany), directly connected to the TSG. Process parameters drying temperature, drying air flow, and dryer rotation speed (i.e. drying time) were varied, to generate granules varying in PSD and LOD (see Section 2.6 for details). Standard process parameters are listed in Section 2.5.

### 2.5. Standard process parameters

Standard process parameters as listed in Table 1 were applied for twin-screw wet granulation and continuous fluid-bed drying, during the performed validation trials on the developed methods (see Section 3.2, page 15 ff.).

All experiments were performed according to the following general procedure: the empty dryer was preheated at the designated drying temperature and airflow rate of 150 $m^3$/h for two hours. Heating of the TSG-barrel at the desired process temperature was started simultaneously. Once the temperature equilibration of the equipment was completed, granulation and drying was started.

### 2.6. Variation in granule characteristics for model development and validation

In total, 102 granule samples for model development were collected from 34 different granulation trials of the described process, during which liquid feed rate (0.65–1.4 kg/h), solid feed rate (2–6 kg/h), screw speed (200–800 rpm), barrel temperature (30–40 °C), drying temperature (65–95 °C), drying air flow (70–150 $m^3$/h), and dryer rotation speed (5–29 rph; corresponding to 9.8–1.7 min drying time [26]) were varied. Samples were selected based on their variations in granule characteristics in PSD, LOD, and API content, as listed in detail in Table 4 (page 10). The developed NIRS methods were further validated for accuracy and robustness towards common process variations, by inducing variations in PSD, LOD, and API content during granulation and drying, and measuring the resulting granules in real-time by NIRS in-line. To induce variations in PSD, the liquid feed-rate during granulation was adapted (at standard solid feed rate and standard drying conditions). For variations in LOD, drying temperature, airflow, and dryer rotation speed were adapted (at standard granulation settings). Details on the applied process parameters are listed in Tables 2 and 3,

**Table 1**
Standard process parameters applied during twin-screw wet granulation and continuous fluid-bed drying.

| Process parameter | Setpoint | Unit |
|---|---|---|
| Solid feed rate | 4 | kg/h |
| Liquid feed rate | 1.2 | kg/h |
| Granulator screw speed | 500 | rpm |
| Granulator barrel temperature | 35 | °C |
| Drying temperature | 80 | °C |
| Drying airflow | 140 | $m^3$/h |
| Dryer rotation speed | 17 | rph |

**Table 2**
Overview of applied liquid feed rates, to induce variations in dried granules PSD (L/S = liquid-to-solid ratio).

| Setpoint # | 1 | 2 | 3 | 4 | 5 |
|---|---|---|---|---|---|
| Liquid feed rate | 0.8 | 0.9 | 1.3 | 1.4 | 1.2 |
| L/S | 0.20 | 0.23 | 0.33 | 0.35 | 0.30 |

**Table 3**
Overview of applied drying conditions, to induce variations in dried granules LOD.

| Setpoint # | 1 | 2 | 3 | 4 | 5 | 6 | 7 | 8 | 9 |
|---|---|---|---|---|---|---|---|---|---|
| Dryer rotation speed | 30 | 30 | 30 | 20 | 20 | 15 | 10 | 8 | 5 |
| Drying air flow | 100 | 80 | 90 | 100 | 110 | 110 | 120 | 140 | 160 |
| Drying temperature | 80 | 80 | 80 | 80 | 80 | 80 | 80 | 80 | 90 |

standard process conditions are listed in Table 1. For variations in API content, powder blends containing 20%, 25%, and 30% of Diclofenac-Na were processed at standard settings (see Section 2.1 for details on the formulation).

### 2.7. Sampling of granules

Dried granules were collected from the dryer outlet in a PE-bag. In total, 102 samples from 34 different granulation trials were collected for analysis. Samples differed in PSD, LOD, and API content, to simulate the limits of potential process variations, according to official guidelines for sample collection in NIRS method development and validation [21–25].

### 2.8. Analysis of water content (LOD)

Sample LOD was analyzed with a loss-on-drying moisture analyzer (HS153, Mettler Toledo, Greifensee, Switzerland), by drying approximately 5 g of granules at 105 °C, until the drying rate was lower than 1 mg/50 s. To avoid bias, sample LOD was first measured directly after sampling and re-measured after NIR offline analysis. In both cases, the sample average LOD and standard deviation (in w/w %) was calculated from three consecutive sample measurements.

### 2.9. Analysis of particle size distribution (PSD)

Sample PSD was measured by dynamic image analysis with a CamSizer XT (Retsch Technology, Haan, Germany) equipped with an X-Jet module operating at 30 kPa dispersion pressure. Volume-based PSDs, calculated from the smallest of all maximum chord lengths of the particle projection (inner width) is reported by the system. Each sample was measured three times with approximately 5 g of granules per measurement, and the average PSD and standard deviation of particle fractions X10, X50, and X90 were calculated for data analysis. Repeatability of the CamSizer measurement was evaluated through the average standard deviation (of the three consecutive analyses per sample) from all samples included into the calibration and validation datasets. Repeatability is further referred to as standard error laboratory (SEL).

### 2.10. Analysis of active pharmaceutical ingredient by HPLC

Content of Diclofenac Sodium in the collected samples was quantified by HPLC with an Agilent 1260 analytical system (Agilent Technologies, Santa Clara, CA, USA), equipped with a 250 × 4.6 mm YMC Pack ODS-AM Column (YMC CO. LTD., Kyoto, Japan). A mixture of Methanol and 0.8 g $NaH_2PO_4 * H_2O$ in water at pH = 2.5 (adjusted with $H_3PO_4$ 85%) was used as mobile phase, with gradient mixing of

35/65 at 0–10 min, 65/35 at 11–30 min, and 35/65 at 31–35 min at a flowrate of 1.5 ml/min. Column temperature was 40 °C, detection wavelength was 254 nm. The sample solvent contained 320 ml tri-sodium citrate dihydrate 1% and 680 ml Ethanol 90%. For sample preparation, 80 mg of dried granules were dissolved ad 100 ml solvent and filtered through a 1 µm glass filter before injection of 40 µl for analysis. Results were corrected for the samples measured LOD. Diclofenac Sodium 99.9% in solvent was used as reference standard.

### 2.11. NIR spectroscopy

NIR spectra were collected with a multichannel diode array NIR spectrometer (SentroPAT FO) in combination with the corresponding measurement probe SentroProbe DR LS (both from Sentronic GmbH, Dresden, Germany). Spectra were collected in diffuse reflectance mode over the spectral range from 1150 to 2100 nm by averaging 60 scans of 0.011 s integration time at a resolution of 2 nm. External referencing was performed before each trial, using a certified 99% reflectance Spectralon® standard. Internal referencing during processing was performed every 30 min with an internal PTFE-wavelength standard located in the measurement probe.

For in-line measurements, the spectrometer was mounted at the outlet of the fluid-bed dryer between two alternating discharge valves, allowing static granule measurement. The probe was in direct contact with the granules during spectral acquisition. The cycle time of the two alternating valves allows static granules measurement for approximately 7 s, before the top valve closes and the lower valve opens to discharge the granules from the dryer for sampling.

For offline NIRS analysis, the probe was directly placed into the granule sample. Depending on the granulation batch and operator, either 50 spectra from ten different positions in the sample were collected (10 × 5 spectra), or 9 spectra from 3 different sample positions (3 × 3 spectra). Due to the availability of the NIRS instrument, in-line spectra were not obtainable for all collected calibration and validation samples.

### 2.12. NIR calibration and validation

In total, 3398 spectra (1513 offline and 1885 in-line) were acquired from 102 samples, originating from 34 different granulation trials. The spectral library was split into a calibration data set (2650 spectra) and a validation data set (748 spectra) for internal validation. Both datasets contained spectra from the same samples, collected from different sample positions (offline spectra) or at different time points (in-line spectra). Additionally, three independent datasets were collected for external method validation and robustness testing against common process variations in LOD and API content. Hence, in-line spectra of continuous granulation and drying trials at varying PSD, LOD, and API content were acquired. These external datasets contained 2865 (PSD variation), 3334 (LOD variation), and 5704 in-line spectra (API content variation).

Three independent methods were created, by calibrating recorded spectra against PSD fractions X10, X50, and X90, respectively. In detail, calibration and validation was performed in several steps, according to common guidelines as described below [21,22,24,25].

#### 2.12.1. PCA analysis and raw spectra assessment

First, raw offline and in-line spectra collected from identical samples were analyzed via principal component analysis (PCA), to evaluate their comparability. PCA is a common qualitative chemometric analysis tool that requires no previous knowledge about the available data. It aims to discover and display object-clusters of related characteristics for exploratory data analysis, by transforming them into a set of new linearly uncorrelated variables called principal components (PCs). Furthermore, spectral baseline offset and slope of raw spectra was correlated to the samples physical and chemical properties particle size, LOD and API content. Spectral slope was calculated from baseline absorbance values at 1320 nm, 1640 nm, and 1810 nm (linear fit).

#### 2.12.2. PLSR analysis, selection of PCs, and investigation of degree of overfit

In a second step, multivariate calibration via partial least squares regression (PLSR) was performed, by fitting three individual models for PSD X10, X50, and X90 to the calibration dataset. PLSR is a quantitative chemometric method that is especially suitable when the number of independent variables is significantly larger than the number of data points in a dataset. In NIR-analysis, PLSR aims to determine the fundamental relations between the instrumental response X and the analyte abundance data Y, with the goal to predict unknown $Y_i$ from new sample spectra $X_i$ [27–29]. Since variance in spectral slope and baseline offset are thought to be desired effects when correlating particle size related information to NIRS spectra, no data preprocessing of raw spectra was performed before PLSR analysis [7,14].

The adequacy of selected number of PCs and degree of overfit was investigated via root mean square error of prediction and -cross validation (RMSEP and RMSECV) and permutation analysis. The models RMSECV and RMSEP as a function of the number of selected PCs, allows the evaluation of predictive power. RMSECV is a common resampling statistic calculated from the calibration data set by the leave-one-out method. RMSEP is based on predictions made from the validation dataset. Permutation analysis is a statistical resampling method that investigates a model's degree of overfit. The datasets y-variables are randomly rearranged for a specified amount of times (here: 20; 20 being the default value suggested by the used software; analyzing more permutations demonstrated to have no significant difference in outcome), and separate models are fitted to all new x–y combinations, containing the same number of PCs as the original model. $R^2$ (coefficient of determination) and $Q^2$ (predictive ability) of permuted models should be significantly lower than of the original model to demonstrate a low degree of overfit [30,31].

#### 2.12.3. Linearity, accuracy, repeatability, and robustness

The selected model's linearity, accuracy and robustness was further assessed as follows. Coefficient of determination $R^2$, bias (calculated as the residual average) and slope of the correlation plot between predicted versus reference values were evaluated for calibration and validation datasets. Generally, good linearity is indicated by $R^2$ and slope as close as possible to 1, and bias and intercept as close as possible to 0 [24,25]. A guideline scale that was specifically developed for NIRS predictive models by Malley et al. [32] considers $R^2 > 0.95$ as successful and $R^2 < 0.7$ as inadequate. Repeatability of NIRS spectral acquisition (and thus, repeatability of NIRS-predictions) was analyzed, by examining the standard deviation between PSD-predictions from five NIRS spectra acquired from the same sample position, as well as PSD-prediction from spectra recorded at three different sample positions.

Furthermore, the ratio of prediction to deviation (RPD), the ratio of prediction error to laboratory error (PRL), and the range error ratio (RER) were evaluated for model assessment. RPD represents the relationship between the variation in sample population and the models prediction error, calculated as the ratio of reference standard deviation and RMSECV or RMSEP. Above cited guideline by Malley et al. [32] considers NIRS models with RPD > 3 successful and RPD < 1.75 inadequate, depending on the intended purpose. PRL represents the ratio of RMSEP or RMSECV to the standard error laboratory SEL (here: calculated from reference repeatability). PRL should be $\leq 2$ for excellent models. RER is calculated as the ratio of calibration sample range (based on reference analytics) and RMSECV or RMSEP. RER $\geq 10$ indicates high model utility, $3 < \text{RER} < 10$ indicates that practical utility is limited [21–25,32,33].

Accuracy and robustness of final models against LOD and API content was demonstrated in-line by three independent, external validation datasets. Predicted in-line NIRS results were compared to reference values from frequently withdrawn samples.

**Table 4**
Variation of granule characteristics in all samples.

| Characteristic | Calibration range | Common process variation[a] |
|---|---|---|
| API content (label claim: 25%) | 17.5–32.5% | ± 5% |
| LOD | 1–11% | ± 0.5% |
| PSD X10 | 20–234 µm | ± 7 µm |
| PSD X50 | 98–1017 µm | ± 28 µm |
| PSD X90 | 748–2297 µm | ± 161 µm |

[a] Common process variation of LOD and PSD X10, X50, and X90 at standard process conditions was quantified in [4]. No published data available for API content; the calibration range was selected based on experience, according to which the common variation is < ± 5% API content.

### 2.13. Software

Sentro Suite package version 2 (Sentronic®, Dresden, Germany) was used for spectra acquisition. Chemometric calibration and validation was performed in SIMCA 13.0.3 (Sartorius-Stedim, Malmö, Sweden).

## 3. Results and discussion

### 3.1. Model development and internal validation

Collected samples for calibration and internal validation were representative of typical variations that might occur in the process. In detail, collected and measured granule samples varied in LOD, PSD and API content; the selected ranges were wider than the actually expected common process variation [4], to ensure a high level of accuracy and robustness. An overview of the selected calibration range and the expected common process variation is presented in Table 4, details on the assessment of the common process variation can be found in [4].

#### 3.1.1. PCA analysis and raw spectra assessment

Comparability of raw offline and in-line spectra in the model data set was assessed by PCA. Score-distribution of in-line spectra was slightly wider, which might be due to larger variation in sample presentation during spectral acquisition. However, the inclusion of both datasets into one model was justified as both score plots overlapped, rather than showing two distinct clusters. Fig. 1 displays the score plot of the first two PCs.

Fig. 2 displays a selection of raw offline and in-line spectra from the calibration data set, colored according to the samples respective X50 value. The main absorption peak of Diclofenac Sodium is found at 1670 nm, the regions between 1400 and 1450 nm and 1900–2000 nm are highly correlated to water absorption. The API's −OH peak at 1930 nm is also detected, but not suitable for analysis due to its close proximity to the water absorption peak [7,11]. The possibility to correlate particle size related information to variances in NIR-spectra is thought to be based on changes in spectral slope and baseline offset, but water content and other sample variations may also play a role in changing those descriptors and need to be considered [7,14,15]. Accordingly, closer inspection of Fig. 2 indicates merely moderate correlation between PSD X50 and the spectral baseline offset. Besides, no significant linear correlation between baseline slope and PSD or LOD or API content was discovered (see supplementary data 6.1 for details). Consequently, as linear correlation of baseline offset or slope demonstrated not sufficient for accurate particle size prediction, PLSR against reference analysis PSD X10, X50, and X90 results was performed, to calibrate three individual regression models.

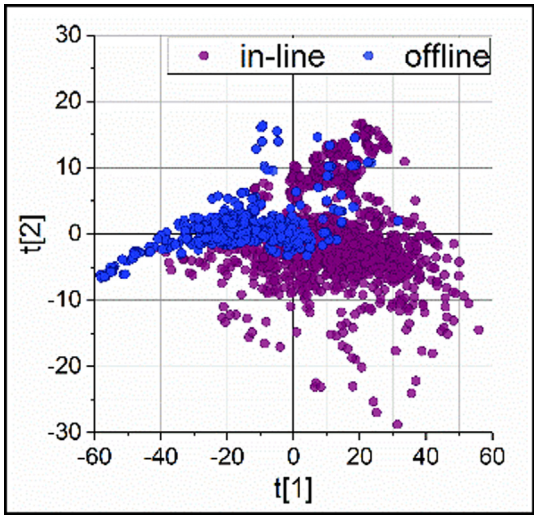


**Fig. 1.** PCA results for PC 1 and 2 of raw offline and in-line spectra in the model data set. Spectra vary in their distribution but sufficient overlap was demonstrated to include both datasets into one model.

#### 3.1.2. PLSR analysis, selection of PCs, and investigation of degree of overfit

PLSR of the calibration data set led to 9 PCs for PSD X10, that represent approximately 85% of the total variance, and 15 PCs for PSD X50 and X90, which represent approximately 75% of the total spectral variance. Generally, to avoid under- or over-fitting of data and to ensure that a model is optimized to its purpose, it is of critical importance to choose the appropriate number of PCs. Loading plots and resampling statistics like cross validation or permutation statistics can aid in this evaluation [24,30,31].

Loading plots visualize the effect of variables X on scores Y for each PC; the respective plots of model PSD X10 are portrayed in Fig. 3. Generally, large positive or negative loadings in the spectral region at 1670 nm indicate spectral variance related to API content, large loadings in the regions between 1400 and 1450 nm and 1900–2000 nm indicate variance related to granules' LOD. Flat plots indicate baseline offsets, and rather noisy plots that do not allow precise attribution of spectral range variability, indicate small local slope and peak changes that are thought to be caused by spectral variability, resulting from physical sample characteristics like particle size, morphology, density, temperature, or sample presentation [11]. Accordingly, Fig. 3 indicates that PC1 was predominantly attributed to the variation in particle size (baseline offset) and PCs 2 and 3 were mainly attributed to the variation in granules LOD and API content (see Fig. 2 for respective absorption regions). PCs 4–9 were added to the model, as no accurate prediction of PSD X10 was possible with only 3 PCs. Their respective loading plots are noisier than the first three loading plots (Fig. 3), suggesting that they contain information about other physical sample variations, that were not primarily related to API content and LOD. This conclusion was in line with Nieuwmeyer et al. [11], who demonstrated that granules of different sizes are described by different spectral variances and therefore by different factors during PLS regression. Since samples originated from numerous different granulation trials, where several process parameters like screw speed, L/S ratio, total material mass flow, drying temperature- and airflow and drying time were varied, numerous small differences in granules' physical properties were expected. The authors decided against thorough, time-consuming analysis of granules physical properties, as validation results reassured the selected number of PCs and no benefit for the NIRS calibration was expected from such analyses (validation results will be provided further below). Loading plots for models PSD X50 and PSD X90 showed similar characteristics and selection of PCs was done in analogy to PSD X10, but 15 PCs were needed in both case for adequate calibration results (see supplementary data 6.2 for loading plots of models PSD X50 and X90 models).

The inclusion of the selected number of PCs into the final models was further justified by statistical testing. Plots of RMSECV and RMSEP in dependence of number of selected PCs demonstrated that each component further decreased the prediction error of the model. In detail, in model PSD X10 RMSEP decreased by approximately 50% from

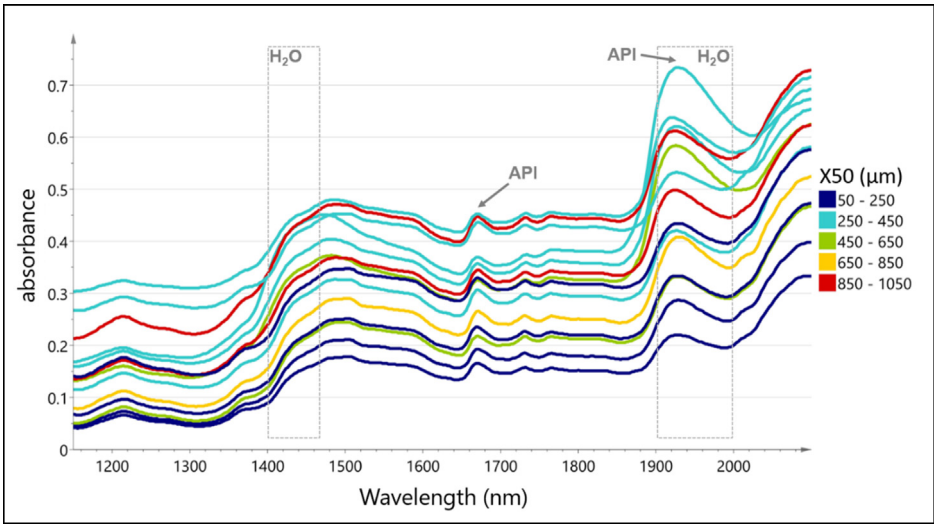


**Fig. 2.** Raw spectra in calibration set, colored according to the samples respective X50 value (µm). (For interpretation of the references to colour in this figure legend, the reader is referred to the web version of this article.)

33 µm (with one PC) to 17 µm (with 9 PCs). In models PSD X50 and X90, RMSEP decreased by approximately 40% from 154 µm to 97 µm (X50 with one PC compared to 15 PCs) and 279 µm to 174 µm (X90 with one PC compared to 15 PCs, see Fig. 4 A-1, B-1, and C-1, respectively). Permutation analysis revealed no model overfitting, as permuted models exhibited no significant $R^2/Q^2$, compared to the original models. Original $R^2/Q^2$ had a correlation of 1 on the x-axis, while the new models had a correlation close to zero. Generally, the intercept of the linear fit between all $R^2/Q^2$ values is considered a measure of overfit; $R^2Y$ intercept should not exceed 0.3–0.4 and $Q^2Y$ intercept should not exceed 0.05 [30,31]. Here, intercepts close to zero were observed for all three models ($R^2Y \leq 0.04$ and $Q^2Y \leq -0.01$ for all three models), indicating no overfitting (see Fig. 4 A-2, B-2, and C-2, respectively).

### 3.1.3. Linearity, accuracy, repeatability, and robustness

Linearity and accuracy was assessed via cross-validation of the calibration data set and the internal validation dataset. For a visual overview, Fig. 5 plots reference values against NIRS-predicted values, and Fig. 6 plots residuals (in % of the reference value) of the validation dataset. Table 5 lists RMSECV/RMSEP, $R^2$, slope, bias, and intercept of calibration and validation results.

$R^2$ of calibration and validation data were comparably low (see Table 5), but values are within the suggested range for adequate NIR calibrations of $0.95 > R^2 > 0.7$ (range according to [32]). Such low coefficients of determination can be explained by the samples appearance in front of the probe during NIRS spectra acquisition: the NIRS-light source scans a sample-area of approximately 4 $mm^2$ per acquired spectrum. Hence, the particle size that is observed by NIRS might fluctuate significantly, depending on the granule population that appears in front of the probe at the instance of spectral acquisition (e.g. due to segregation within the measurement cell). In contrast, during reference CamSizer analysis, 5 g of sample are measured three times, giving a reasonable average description of the whole sample population. As one average reference values for PSD X10, X50, and X90 was then calibrated to a series of spectra taken in different positions of the same sample, variabilities in PSD-prediction were to be expected (This hypothesis was also confirmed by analyzing the NIRS prediction repeatability: five spectra acquired from the same sample position resulted in repeatability of ± 0.7 µm, ± 16 µm, and ± 32 µm; while repeatability between three different sample positions (within the same sample) was ± 6 µm, ± 32 µm, and ± 58 µm, for PSD X10, X50, and X90, respectively.

Furthermore it was observed that residuals from offline spectra were slightly higher than residuals from in-line spectra (see Fig. 6). This might be due to different sample presentation during offline spectral acquisition (compared to in-line spectral acquisition) and also due to the above discussed influence of the small NIRS measurement area in

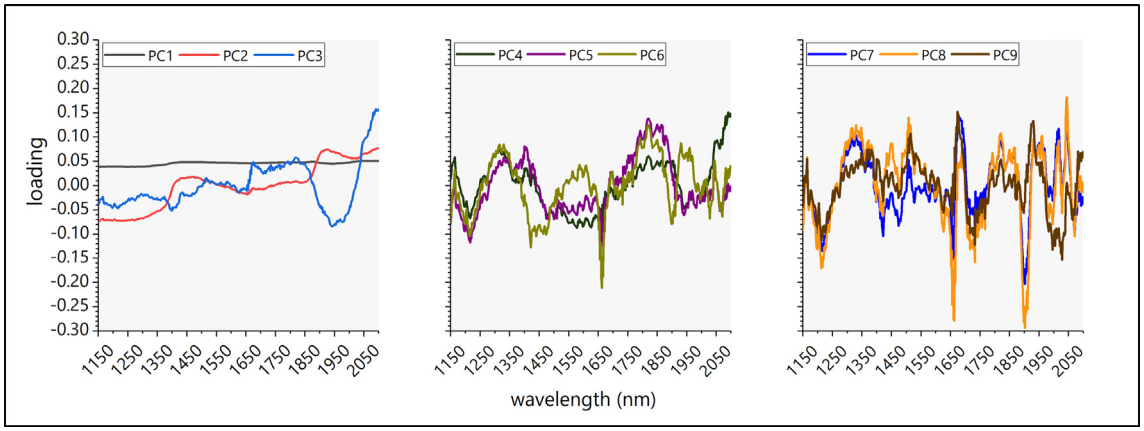


**Fig. 3.** Loading plots of model PSD X10 (9 PCs). PC1 was attributed to the samples' variations in particle size and PCs 2 and 3 are mainly attributed to variations in granules LOD and API content. PCs 4–9 include additional spectral variances into the model that were not covered by the first three components.

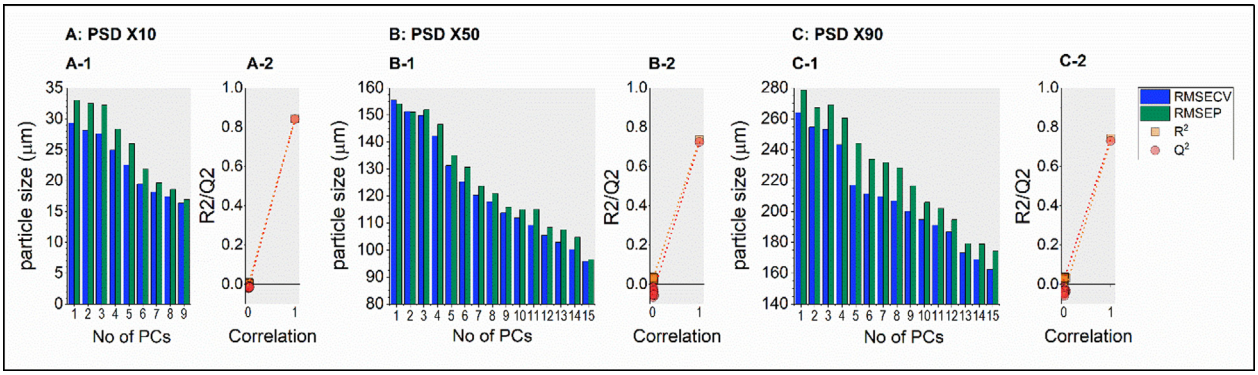


**Fig. 4.** A-1, B-1, C-1: RMSECV and RMSEP as a function of the number of PCs for models PSD X10, X50, X90, respectively. Each selected component further decreased RMSECV/RMSEP and thus increased the predictive power of the model. A-2, B-2, C-2: permutation analysis with 20 permutations of models PSD X10, X50, X90.

relation to the granule particle size and the measured granule population in front of the probe when analyzing granules from different sample positions.

In detail, RMSEP was 17 µm, 97 µm, and 174 µm for PSD X10, X50, and X90, respectively (see Table 5). In comparison, CamSizer SEL was found to be ± 8 µm, ± 59 µm, and ± 128 µm for PSD X10, X50, and X90. As the RMSEP represents the sum of all individual variances that influence the model (e.g. reference analysis variance (SEL), NIRS analysis variance, and sample variance, etc.) it was expected to be larger than SEL. However, as prediction errors were all within the suggested range of two times the standard laboratory error (PRL), acceptable accuracy of the NIRS method in relation to the reference method was demonstrated. Also, the ratios of calibration sample range (based on reference analytics) to prediction errors reached the accepted limit of RER ≥ 10, which indicates high model utility. And, despite of rather low $R^2$ and high residuals, the range of sample population variation to the models prediction error (RPD) was within the accepted range for adequate NIRS methods (3 < RPD < 1.75) for all models (see Table 5). In summary, internal model validation demonstrated that the developed models have acceptable accuracy and precision for the intended purpose to observe sudden variations and trends in granules PSD after continuous granulation and fluid bed drying.

### 3.2. External model validation and robustness testing with in-line data

Common variations in the described granulation and drying process can occur mainly in regard to dried granules LOD and PSD (e.g. due to external process disturbances, common deviations in feeding behavior, or granulation behavior) [4]. Furthermore, if API and excipients are supplied by individual feeders, or if drug products at different dosage strengths are to be produced, variations in API content may also occur. Consequently, the developed methods should demonstrate robustness towards these variations, while accurately predicting the dried granules PSD. Consequently, to test the methods accuracy and robustness towards LOD and PSD, three external validation trials were performed.

In the first trial, the methods accuracy in-line was demonstrated by varying dried granules' PSD over time through the adaption of the materials liquid-to-solid ratio (L/S) during wet-granulation (at constant drying parameters). In the second trial, the methods robustness against LOD variations was demonstrated by varying LOD at constant PSD, through the adaption of drying temperature, air-flow and dryer rotation speed, i.e. residence time (at constant L/S ratios). In the third validation trial, the methods robustness against varying API content was demonstrated by granulating powder blends containing 20%, 25%, and 30% of API at constant LOD and PSD.

Fig. 7 summarizes the results of the first validation trial, where wet granules L/S ratio (Fig. 7, A) was plotted in relation to in-line NIRS-predicted values and reference analysis results (Fig. 7, B). The length of the red bar indicates the sampling time; the error bar indicates the standard deviation of three consecutive reference analyses. The results demonstrated that the developed NIRS-methods can accurately monitor occurring trends and sudden changes in dried granules' PSD-fractions X10, X50, and X90 in-line in real-time, as each performed step-change in L/S ratio was clearly indicated by NIRS. The observed variability in predicted particle size can be explained by the size of the NIRS measurement area in relation to particle size and the variability in sample presentation in front of the probe, as explained already during internal method validation. This effect could be smoothed out by applying a box filter or similar averaging approach to the control plot. The observed small deviations between reference and NIRS prediction were perceived as acceptable, as the methods intention was trend monitoring, not precise prediction of granules PSD.

Granule PSD is highly correlated to wet granules L/S ratio and hence, dried granules LOD [4]. To avoid prediction errors in PSD,

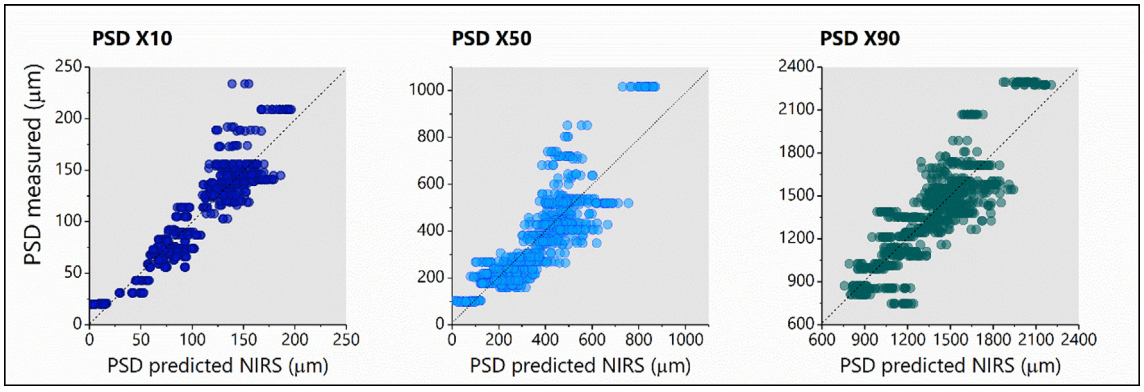


**Fig. 5.** Observed vs. predicted plot of validation dataset gives a visual overview of slope, bias and intercept of the three models.

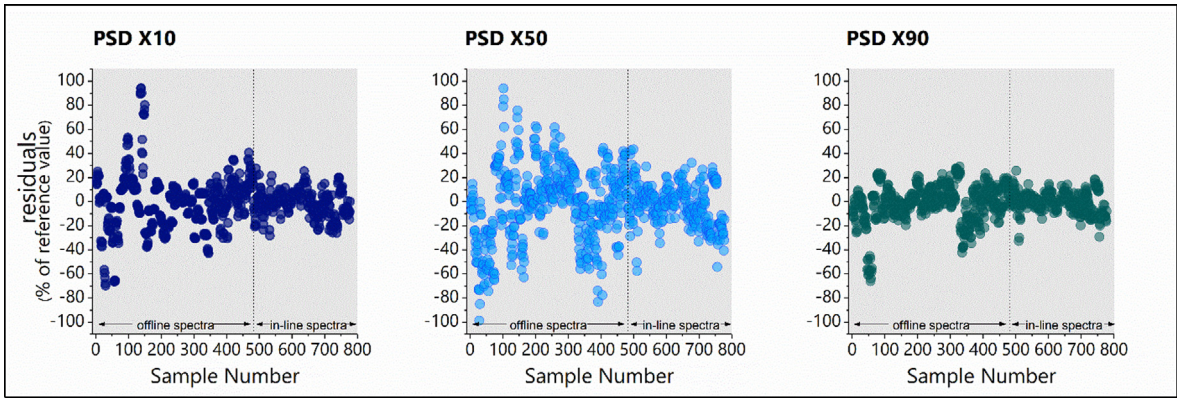


**Fig. 6.** Residuals in the validation data set are comparable between offline and in-line spectra.

**Table 5**
Summary of calibration and internal validation.

| | PSD X10 | PSD X50 | PSD X90 |
|---|---|---|---|
| *Calibration set* | | | |
| RMSECV (µm) | 16 | 96 | 162 |
| $R^2$ | 0.85 | 0.75 | 0.76 |
| Slope | 1 | 1 | 1 |
| Bias (µm) | $-1*10^{-6}$ | $1*10^{-4}$ | $2*10^{-4}$ |
| Intercept (µm) | $5*10^{-7}$ | $1*10^{-4}$ | $2*10^{-3}$ |
| RPD | 3 | 2 | 2 |
| PRL | 2 | 2 | 1 |
| RER | 13 | 10 | 10 |
| *Validation set* | | | |
| RMSEP (µm) | 17 | 97 | 174 |
| $R^2$ | 0.86 | 0.73 | 0.74 |
| Slope | 0.99 | 0.98 | 0.99 |
| Bias (µm) | −0.05 | 2.45 | 5.12 |
| Intercept (µm) | 1.01 | 8.78 | 18.99 |
| RPD | 3 | 2 | 2 |
| PRL | 2 | 2 | 1 |
| RER | 13 | 10 | 10 |

caused by variations in LOD (e.g. triggered by variations in drying efficiency or liquid feed rate during granulation), the methods robustness towards LOD was demonstrated in the second external validation trial. Fig. 8 plots dried granules' LOD (based on reference analytics, see Fig. 8, A) in relation to in-line NIRS- and offline reference results (Fig. 8, B). Dried granules' LOD varied between approximately 2% and 11%. However, NIRS predictions of PSD X10, X50, and X90 were in close agreement with the reference results throughout the trial, demonstrating good robustness against LOD variations.

In the future, API and excipients will be fed separately into a continuous blender, before the blend enters the TSG. Hence, variations in API can occur, and it needs to be ensured that the developed NIRS methods for PSD, are not affected by such variations. Consequently, the methods robustness towards varying API content was demonstrated in a third validation trial, where blends containing variable amounts of API were granulated and dried and then analyzed by NIRS in-line. Fig. 9 plots in-line NIRS-predicted PSD of granules containing 20%, 25% and 30% of API in comparison to offline reference PSD results. The results demonstrate, that the granules' API content did not bias NIRS predictions; close agreement with the reference PSD analysis was found. Hence, robustness towards variations in API content was demonstrated.

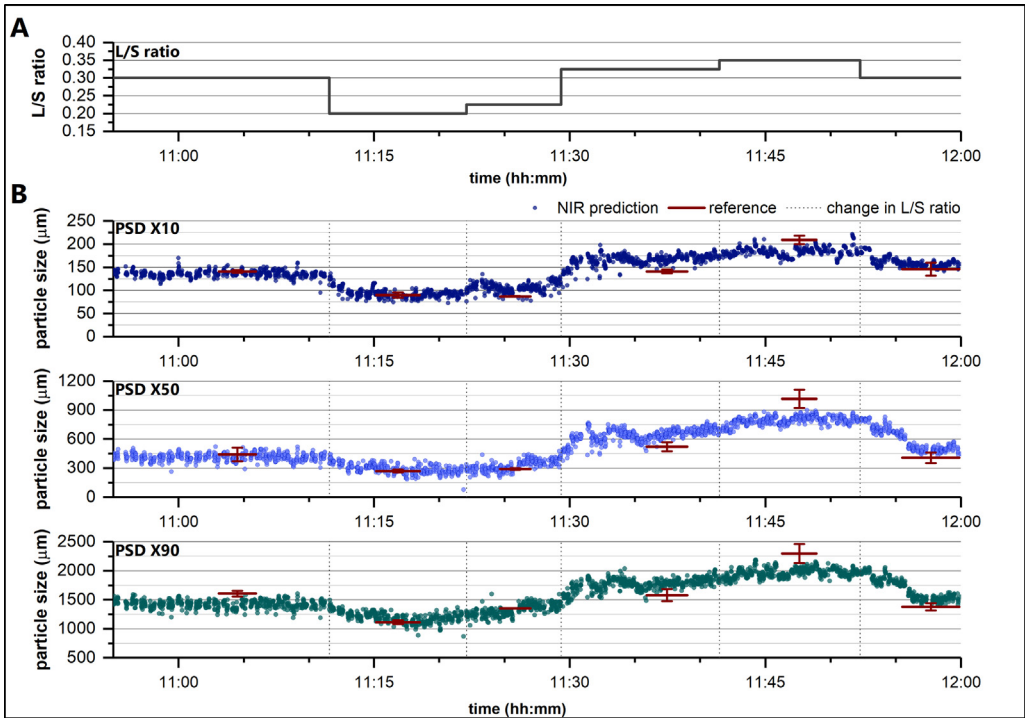


**Fig. 7.** External in-line validation I. A: L/S ratio during wet-granulation (for a better visual comparison, the time axis was corrected for the mean residence time of the granules in the dryer, i.e. the graph displays the theoretical L/S ratio the granules would have at the time point of exiting the dryer, if no drying occurred). B: NIRS-predicted PSD X10, X50, and X90 compared to reference PSD results. The length of the red bar indicates the sampling time; the error bar indicates the standard deviation of three consecutive reference analyses. (For interpretation of the references to colour in this figure legend, the reader is referred to the web version of this article.)

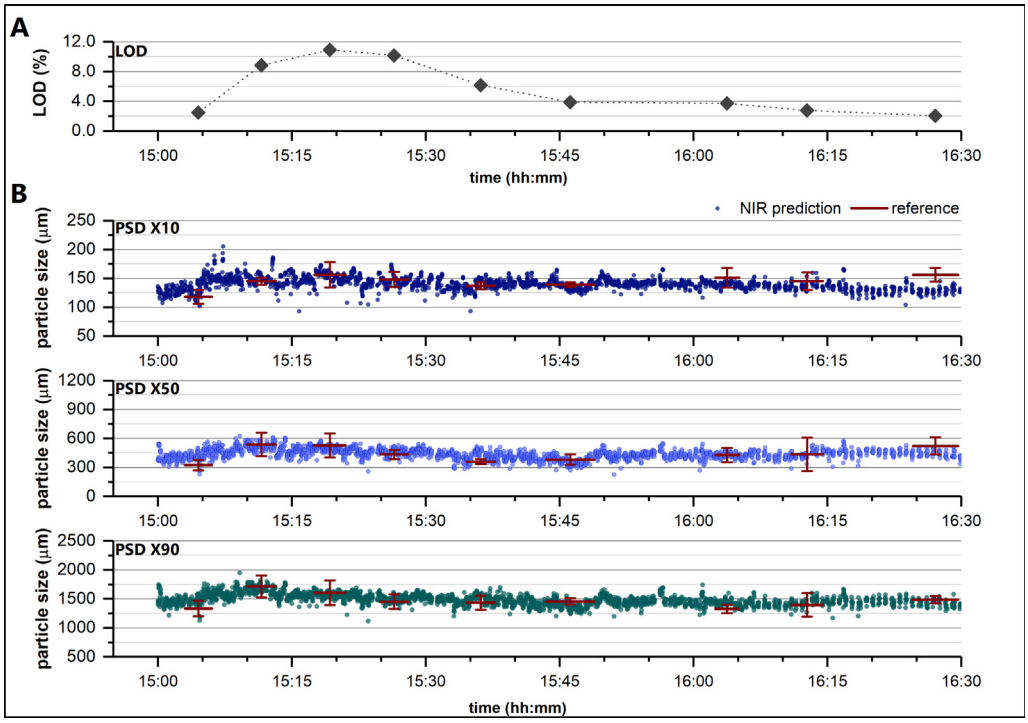


**Fig. 8.** External in-line validation II: the methods robustness against variations in dried granules LOD was demonstrated by intentionally varying LOD through the adaption of drying conditions. A: dried granules' LOD measured by reference analytics. B: NIRS-predicted PSD compared to reference PSD results (X10, X50, and X90, respectively). The length of the red bar indicates the sampling time; the error bar indicates the standard deviation of three consecutive reference analyses. (For interpretation of the references to colour in this figure legend, the reader is referred to the web version of this article.)

## 4. Summary and conclusion

PSD is a critical quality attribute in the investigated CM-process, as it can directly influence subsequent downstream manufacturing steps: too large granules can cause insufficient die-filling during tableting, too many fines in the granules can cause sticking in the tablet press or negatively influence the final quality characteristics. Such variations can be caused by internal or external process disturbances (e.g. over-wetting in the granulator, varying drying conditions caused by variations in drying inlet humidity, etc.), that cannot be avoided at all times. CM in combination with suitable PAT offers the potential to respond to such variations in real-time, through the appropriate adaption of process conditions.

In this context, three NIRS methods for analysis of particle size fractions X10, X50, and X90 were developed as a suitable PAT-approach to monitor trends and sudden changes in granules PSD in real-time. Methods demonstrated good accuracy, and robustness towards common process variations like sample LOD or API content.

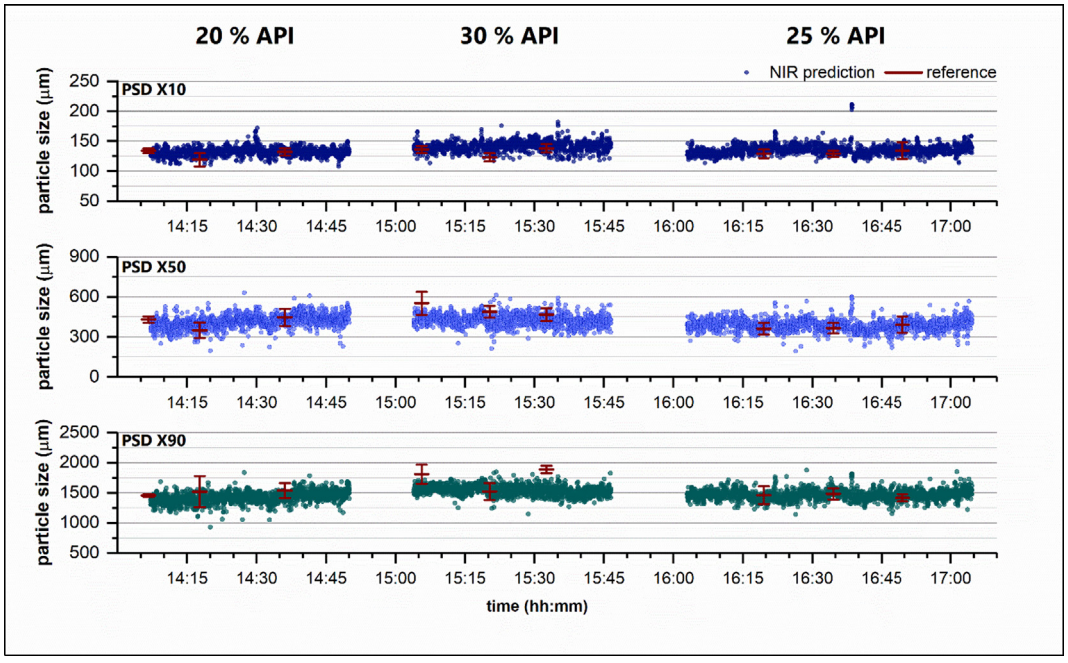


**Fig. 9.** External in-line validation III: the methods robustness against variations in API-content was demonstrated. A-C: NIRS-predicted PSD compared to reference PSD results (X10, X50, and X90, respectively) at varying API content between 20% and 30%. The length of the red bar indicates the sampling time; the error bar indicates the standard deviation of three consecutive reference analyses. (For interpretation of the references to colour in this figure legend, the reader is referred to the web version of this article.)

In detail, PLSR of raw NIRS spectra resulted in the independent methods with RMSEP 17 µm, 97 µm, and 174 µm, for particle size fractions X10, X50, and X90, respectively. RPD, PRL, and RER were evaluated to judge the created models; with all values within the acceptance range for adequate to good NIR methods ($1.75 < RPD < 3$, $PRL \leq 2$, $RER \geq 10$). The diverse sample populations that were included into the calibration models, justified the inclusion of a large number of PCs that cannot be fully attributed to identified sample variations; loading plots and permutation analysis confirmed that the number of selected PCs was appropriate to describe and predict the occurring variation in granule size without overfitting the model. Thorough external method validation with three independent in-line datasets further demonstrated the methods applicability to accurately monitor granules PSD in-line, during routine granulation and drying processes. The methods robustness against common process variations in LOD and API content was also demonstrated. Robustness towards LOD was important, as PSD is highly correlated to LOD. Hence, occurring process variations in LOD could suggest PSD variations, if the method has poor robustness. Variations in API content can occur in a CM process where API and excipients are supplied by individual feeders to the manufacturing line. Hence, it needs to be ensured that PSD is monitored, independent of the API content of the observed material.

In summary, the presented NIRS-methods for the monitoring of particle size fractions X10, X50, and X90, proved to be a beneficial PAT-tool in pharmaceutical continuous manufacturing of tablets via twin-screw wet-granulation. All samples and NIRS data used for the calibration were collected from technical trials and DoEs that were anyways performed during routine process development of the described process and product. Hence, no additional lab trials were required; solely data analysis and sample reference analysis had to be performed on top. External in-line validation was done by three individual trials that required a bit of dedicated work, in addition to standard development activities. However, such method validation could also be combined with process validation or control strategy validation trials, which has to be performed in any case. As NIRS methods are highly product specific, the calibration needs to be re-validated, adjusted, or even repeated, in case of formulation change or product change.

Overall, the method will aid in increasing the operators process knowledge and improve process control, without the need for new capital investments, in cases where NIRS is already established as a common PAT-tool in CM (e.g. when already applied to measure granules' LOD or API content). In a next step, the developed PAT methods will be combined with real-time compensatory control actions, to evaluate how they could aid in minimizing or even preventing process-issues and the production of out-of-specification product.

## Declaration of Competing Interest

None.

## Appendix A. Supplementary material

Supplementary data to this article can be found online at https://doi.org/10.1016/j.ejpb.2019.05.007.

## References


[1] R. Meier, M. Thommes, N. Rasenack, et al., Granule size distributions after twin-screw granulation – do not forget the feeding systems, Eur. J. Pharm. Biopharm. 106 (2016) 59–69, https://doi.org/10.1016/j.ejpb.2016.05.011.

[2] J. Litster, B. Ennis, The Science and Engineering of Granulation Processes, Springer, Netherlands, Dordrecht, Netherlands, 2004, , https://doi.org/10.1007/978-94-017-0546-2.

[3] M.A. Alam, Z. Shi, J.K. Drennen, et al., In-line monitoring and optimization of powder flow in a simulated continuous process using transmission near infrared spectroscopy, Int. J. Pharm. 526 (2017) 199–208, https://doi.org/10.1016/j.ijpharm.2017.04.054.

[4] V. Pauli, F. Elbaz, M. Krumme, et al., Methodology for a variable rate control strategy development in continuous manufacturing applied to twin-screw wet-granulation and continuous fluid-bed drying, J. Pharm. Innov. 13 (2018) 247–260, https://doi.org/10.1007/s12247-018-9320-6.

[5] A. Kumar, J. Vercruysse, M. Toiviainen, et al., Mixing and transport during pharmaceutical twin-screw wet granulation: experimental analysis via chemical imaging, Eur. J. Pharm. Biopharm. 87 (2014) 279–289, https://doi.org/10.1016/j.ejpb.2014.04.004.

[6] T. Monteyne, J. Vancoillie, J.-P. Remon, et al., Continuous melt granulation: influence of process and formulation parameters upon granule and tablet properties, Eur. J. Pharm. Biopharm. 107 (2016) 249–262, https://doi.org/10.1016/j.ejpb.2016.07.021.

[7] E.M. Hansuld, L. Briens, A review of monitoring methods for pharmaceutical wet granulation, Int. J. Pharm. 472 (2014) 192–201, https://doi.org/10.1016/j.ijpharm.2014.06.027.

[8] A. Burggraeve, T. Van Den Kerkhof, M. Hellings, et al., Evaluation of in-line spatial filter velocimetry as PAT monitoring tool for particle growth during fluid bed granulation, Eur. J. Pharm. Biopharm. 76 (2010) 138–146, https://doi.org/10.1016/j.ejpb.2010.06.001.

[9] A. Burggraeve, T. Monteyne, C. Vervaet, et al., Process analytical tools for monitoring, understanding, and control of pharmaceutical fluidized bed granulation: a review, Eur. J. Pharm. Biopharm. 83 (2013) 2–15, https://doi.org/10.1016/j.ejpb.2012.09.008.

[10] R. Liu, L. Li, W. Yin, et al., Near-infrared spectroscopy monitoring and control of the fluidized bed granulation and coating processes – a review, Int. J. Pharm. 530 (2017) 308–315, https://doi.org/10.1016/j.ijpharm.2017.07.051.

[11] F.J.S. Nieuwmeyer, M. Damen, A. Gerich, et al., Granule characterization during fluid bed drying by development of a near infrared method to determine water content and median granule size, Pharm. Res. 24 (2007) 1854–1861, https://doi.org/10.1007/s11095-007-9305-5.

[12] T. De Beer, A. Burggraeve, M. Fonteyne, et al., Near infrared and Raman spectroscopy for the in-process monitoring of pharmaceutical production processes, Int. J. Pharm. 417 (2011) 32–47, https://doi.org/10.1016/j.ijpharm.2010.12.012.

[13] M. Alcalà, M. Blanco, M. Bautista, et al., On-line monitoring of a granulation process by NIR spectroscopy, J. Pharm. Sci. 99 (2010) 336–345, https://doi.org/10.1002/jps.21818.

[14] H.W. Siesler, Y. Ozaki, S. Kawata, H.M. Heise (Eds.), Near-Infrared Spectroscopy: Principles, Instruments, Applications, WILEY-VCH Verlag GmbH, Weinheim, Germany, 2002ISBN 978-3-527-30149-2.

[15] A.C. Jørgensen, P. Luukkonen, J. Rantanen, et al., Comparison of torque measurements and near-infrared spectroscopy in characterization of a wet granulation process, J. Pharm. Sci. 93 (2004) 2232–2243, https://doi.org/10.1002/jps.20132.

[16] J. Rantanen, J. Yliruusi, Determination of particle size in a fluidized bed granulator with a near infrared set-up, Pharm. Pharmacol. Commun. 4 (1998) 73–75.

[17] W. Paul Findlay, G.R. Peck, K.R. Morris, Determination of fluidized bed granulation end point using near-infrared spectroscopy and phenomenological analysis, J. Pharm. Sci. 94 (2005) 604–612, https://doi.org/10.1002/jps.20276.

[18] J.G. Rosas, M. Blanco, J.M. González, et al., Real-time determination of critical quality attributes using near-infrared spectroscopy: a contribution for Process Analytical Technology (PAT), Talanta 97 (2012) 163–170, https://doi.org/10.1016/j.talanta.2012.04.012.

[19] M. Otsuka, Y. Mouri, Y. Matsuda, Chemometric evaluation of pharmaceutical properties of antipyrine granules by near-infrared spectroscopy, AAPS PharmSciTech 4 (2003) 142–148, https://doi.org/10.1208/pt040347.

[20] A.T. Tok, X. Goh, W.K. Ng, et al., Monitoring granulation rate processes using three PAT tools in a pilot-scale fluidized bed, AAPS PharmSciTech 9 (2008) 1083–1091, https://doi.org/10.1208/s12249-008-9145-6.

[21] Chapter 2.2.40. Near-infrared spectroscopy (01/2014:20240), in: European Pharmacopoeia 9.5, Council of Europe, Strasbourg, 2018, pp. 64–69.

[22] Chapter 5.21. Chemometric methods applied to analytical data (04/2016:52100), in: European Pharmacopoeia 9.5, Council of Europe, Strasbourg, 2018, pp. 783–800.

[23] Analytical procedures and methods validation for drugs and biologics, in: Guidance for Industry, Food and Drug Administration (FDA), 2015, Available from: < https://www.fda.gov/downloads/drugs/guidances/ucm386366.pdf > .

[24] Guideline on the use of near infrared spectroscopy by the pharmaceutical industry and the data requirements for new submissions and variations in: Scientific Guidelines, European Medicines Agency, 2014, Available from: < http://www.ema.europa.eu/docs/en_GB/document_library/Scientific_guideline/2012/02/WC500122769.pdf > .

[25] C. Vervaet, J.P. Remon, Continuous granulation in the pharmaceutical industry, Chem. Eng. Sci. 60 (2005) 3949–3957, https://doi.org/10.1016/j.ces.2005.02.028.

[26] V. Pauli, F. Elbaz, M. Krumme, et al., Orthogonal redundant monitoring of a new continuous fluid-bed dryer for pharmaceutical processing by means of mass and energy balance calculations and spectroscopic techniques, J. Pharm. Sci. (2019), https://doi.org/10.1016/j.xphs.2018.12.028.

[27] N.L. Calvo, R.M. Maggio, T.S. Kaufman, Characterization of pharmaceutically relevant materials at the solid state employing chemometrics methods, J. Pharm. Biomed. Anal. 147 (2018) 538–564, https://doi.org/10.1016/j.jpba.2017.06.017.

[28] P. Geladi, B.R. Kowalski, Partial least-squares regression: a tutorial, Anal. Chim. Acta 185 (1986) 1–17, https://doi.org/10.1016/0003-2670(86)80028-9.

[29] T. Hastie, R. Tibshirani, J. Friedmann, The Elements of Statistical Learning, second ed., Springer-Verlag, New York, 2009.

[30] User Guide to SIMCA – Version 13, in: MKS data analytics, MKS Umetrics, Malmö, Sweden, 2012.

[31] L. Eriksson, T. Byrne, E. Johansson, et al., Multi- and Megavariate Data Analysis: Basic Principles and Applications, third ed., MKS Umetrics, Umea, Sweden, 2013.

[32] D. Malley, P.D. Martin, E. Ben-Dor, Application in analysis of soils, in: C.A. Roberts, J. Workman Jr, J.B. Reeves (Eds.), Near infrared spectroscopy in agriculture, American Society of Agronomy, Crop Science Society of America, and Soil Science Society of America, Madison, USA, 2004, ISBN: 0-89118-155-5.

[33] Z. Yang, G. Nie, L. Pan, et al., Development and validation of near-infrared spectroscopy for the prediction of forage quality parameters in Lolium multiflorum, PeerJ 5 (2017) e3867, , https://doi.org/10.7717/peerj.3867.